ELSEVIER

Biochimica et Biophysica Acta 1538 (2001) 28–37

BIOCHIMICA ET BIOPHYSICA ACTA

BBA

www.elsevier.com/locate/bba

Electrical stimulation influences mineral formation of osteoblast-like cells in vitro

Hans-Peter Wiesmann [a,*], Mareke Hartig [a], Udo Stratmann [b], Ulrich Meyer [a], Ulrich Joos [a]

[a] *Biomineralization research unit, Klinik und Poliklinik für Mund- und Kiefer-Gesichtschirurgie der Universität Münster, Waldeyerstrasse 30, 48149 Münster, Germany*

[b] *Biomineralization research unit, Institut für Anatomie der Universität Münster, Vesaliusweg 2–4, 48129 Münster, Germany*

Received 15 August 2000; received in revised form 28 November 2000; accepted 29 November 2000

Abstract

The aim of the present study was to assess the structure of newly formed mineral crystals after electrical stimulation of osteoblast-like cells in vitro. Pulsed electrical stimulation was coupled capacitively or semi-capacitively to primary osteoblast-like cells derived from bovine metacarpals. Computer calculations revealed that the chosen input signal (saw-tooth, 100 V, 63 ms width, 16 Hz repetition rate) generated a short pulsed voltage drop of 100 μV (capacitive coupled mode) and of 350 μV (semi-capacitive coupled mode) across the cell-matrix layer. Stimulated cultures showed an enhanced mineral formation compared to the non stimulated controls. In cultures exposed to capacitively coupled electric fields and in control cultures nodules and mineralized globules were found. Nodules with a diameter of less than 200 nm covered the cell surface, whereas mineral globules with a diameter of up to 700 nm formed characteristic mineral deposits in the vicinity of the cells similar to biomineral formations occurring in mineralizing tissues. In contrast, large rod-shaped crystals were found in cultures stimulated by semi-capacitive coupled electric fields, indicating a non-physiological precipitation process. In conclusion, osteoblasts in culture are sensitive to electrical stimulation resulting in an enhancement of the biomineralization process.

Keywords: Apatite; Mineralization; Electrical stimulation; Cell culture

1. Introduction

The discovery of the electromechanical properties of bone in the 1950s led to the hypothesis, that the biological reactions of bone are dependent on its electromechanical potentials [1,2]. Thus, acceleration of bone healing by electrical stimulation has been demonstrated by in vivo studies in a series of publications [3–9]. The factors that trigger the multistep process of biomineralization of osseous repair tissue with the underlying mechanism of the healing process at the cellular and subcellular level is still unknown. Particularly, the influence of electrical stimulation on the sequential development of osteoblast differentiation and mineral formation has not yet been clarified. Several in vitro bone cell studies have been performed with the attempt of characterizing electrically induced molecular–biological and cytobiological reactions [10–15] but none of these investigations has focused on mineral formation.

The present study was designed to explore the

* Corresponding author. Fax: +49-251-835-5143.

0167-4889/01/$ – see front matter
PII: S0167-4889(00)00135-X

mineral structure of mineralizing osteoblast cell cultures that were electrically stimulated by capacitively and semi-capacitively coupled electric pulses, respectively.

2. Materials and methods

2.1. Cell culture

Osteoblast-like cells were derived from the periosteal layer of calf metacarpals. The periost was cut into pieces of 3–6 mm and were transferred to culture dishes with the osteogenic layer facing downwards. Osteoprogenitor cells migrate from the tissue explants as described by Jones and Boyde [16]. Explants were cultured for 3 weeks in High Growth Enhancement Medium (ICN Biomedicals, Eschwege, Germany) supplemented with 10% fetal calf serum, 250 μg/ml amphotericin B, 10 000 IU/ml penicillin, 10 000 μg/ml streptomycin, 200 mM L-glutamine (Biochrom KG seromed, Berlin, Germany) at 37°C and 5% CO_2 in humidified air. Medium was replaced once a week.

For plating, primary cells were harvested by successive incubation in collagenase (Biochrom KG seromed) in Tyrode solution and subsequently pelleted by centrifugation. An aliquot was retained for the determination of cell number and cell size using a coulter counter system (CASY I Model TT, Schärfe System, Reutlingen, Germany). Resuspended cells were inoculated on culture dishes at a density of 5.5×10^4 cells/cm^2 and cultured for up to 21 days. For mineralization experiments, 10 mM β-glycerophosphate was added to the culture medium.

Cell morphology was continuously monitored by phase-contrast light microscopy. Furthermore, cells were characterized by determination of alkaline phosphatase (AP) activity (Alkaline Phosphatase Substrate kit III, Vector Laboratories, Burlingame, CA) and by immunodetection of bone matrix associated proteins using monoclonal anti-osteocalcin, anti-osteonectin, anti-procollagen type I (Takara Biomedical Europe, Gennevilliers, France), anti-collagen type I (Sigma–Aldrich), anti-collagen type II (Biogenesis, Poole, UK) and anti-bone sialoprotein (ImmunDiagnostik, Bensheim, Germany) antibodies. For determination of bone matrix proteins and AP activity, medium was decanted and the adherent cell monolayer was washed with phosphate-buffered saline (PBS) prior to immunostaining. AP-measurement and immunodetection of electrically stimulated as well as control cultures was carried out on day 7 (before onset of electrical pulse application) and on day 21 (after 14 days electrical pulse application).

2.2. Electrical stimulation

Electrical stimulation was started 7 days after plating and was terminated at day 21. Two different modes of stimulation were continuously applied for a period of 2 weeks, i.e., the capacitive coupling mode and the semi-capacitive coupling mode of electric pulses. In the capacitively coupled mode both electrodes were placed outside the culture medium whereas in semi-capacitively coupled model one electrode was immersed into the culture medium. The experimental set-up is shown in Fig. 1. Pairs of circular high-grade steel electrodes constituted the electrical capacitors. Culture dishes were placed between these electrodes. The lower electrode was isolated from the medium by the polystyrene bottom of the culture dish. For capacitive coupling the upper electrode was positioned above the medium leaving an air gap of approximately 1 mm, whereas the upper electrode just touched the medium for the semi-capacitive coupling mode. Up to 12 of these capacitors were arranged in a CO_2-incubator allowing simultaneous long-term field applications to several culture dishes.

In order to optimize electrical stimulation parameters, computer simulations (ICAP/4Windows, Intusoft, San Pedro, CA) were performed to characterize the electric fields generated across the cells. Our simulation-model of the experimental setup takes into account the various components of the plate capacitor system, i.e.: the polystyrene bottom of the culture dish, the adherent cell monolayer, the culture medium, and the air gap separating the upper electrode from the medium (for the capacitive coupling mode). Based on theoretical data and experimental values for capacitance and resistance, the wiring diagram depicted in Fig. 1B was developed.

For electrical stimulation an asymmetric saw-tooth voltage (63 ms width, 16 Hz repetition rate) with a peak-to-peak (pp) amplitude of 100 V at the capaci-

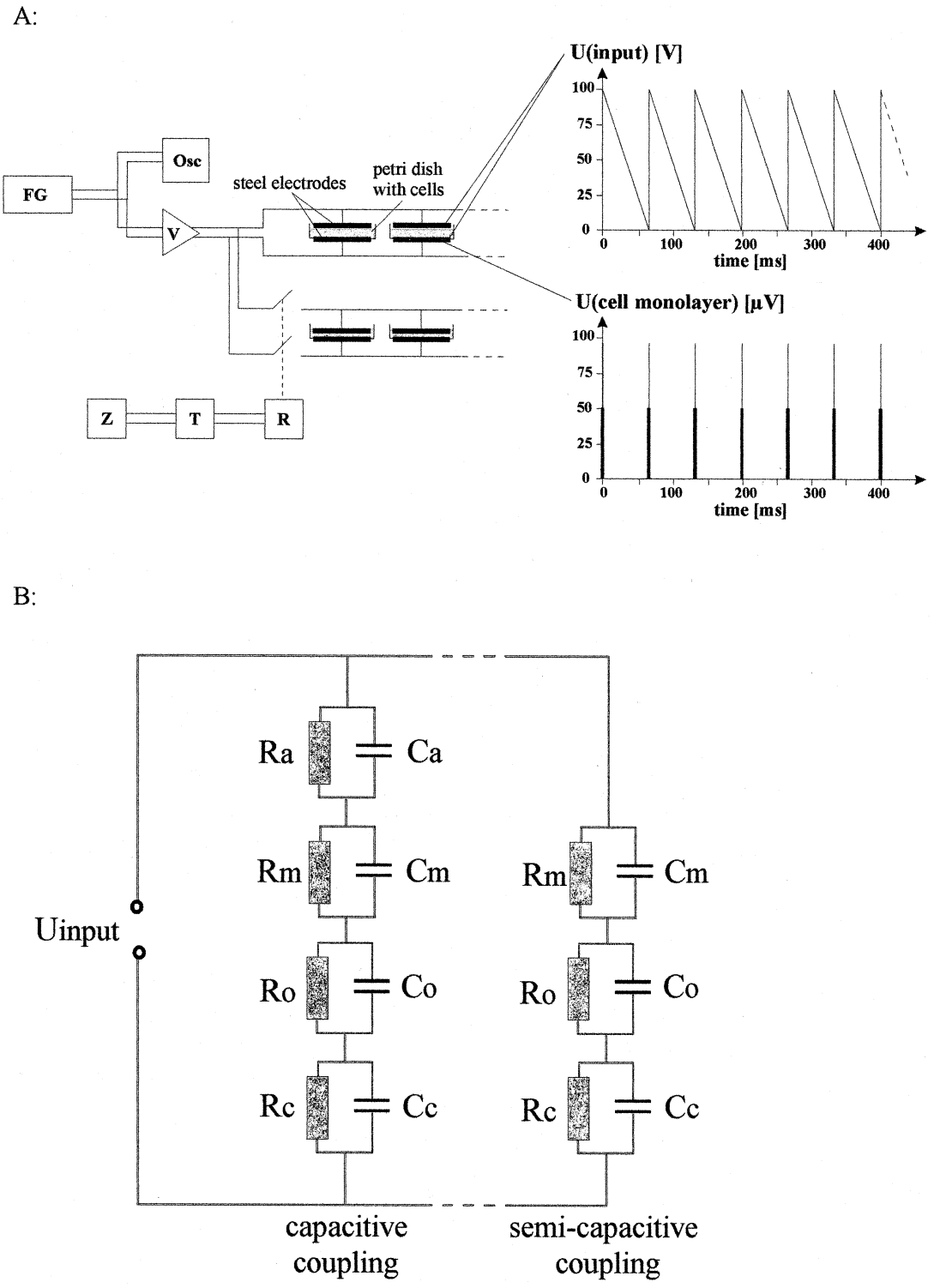

tor was applied leading to a voltage drop across the cell monolayer of 100 µV (corresponding to an electrical field of 6 kV/m) for the capacitive coupling mode (Fig. 1B, right side) and a voltage drop of 350 µV (corresponding to an electrical field of 21 kV/m) for the semi-capacitive coupling mode (signal not shown). These electrical field strengths are similar to other studies [10]. Signals were generated from

Fig. 1. (A) Experimental setup for electrical field application. The system is fed by a function generator (FG) generating specified signals being visualized on an oscilloscope (Osc). Input signals of 5 Vpp are amplified by a voltage amplifier (V) resulting in 100-Vpp signals at the parallel-connected capacitors. The culture dishes containing the cultures are placed between the pairs of electrodes and were electrically stimulated in two different modes, by capacitively coupled electric fields (upper electrode positioned above the medium leaving an air gap) and by semi-capacitively coupled electric fields (upper electrode in contact with the medium). Using a timer (Z), a transformer (T) and a relay (R) different periods of time of voltage application could be realized. The right side of the figure shows the curve of the voltage U(cell monolayer) across the monolayer (below) in response to an external saw-tooth signal U(input) of 100 Vpp at the capacitors (above) with a repetition rate of 16 Hz ($\sim$63 ms period). Calculation is based upon the experimental setup depicted in B. (B) Wiring diagram representing the experimental setup. Separate RC-circuits characterize the electrical features of the polystyrene bottom of the culture dish (Rc,Cc), of the adherent osteoblast monolayer (Ro,Co), of the culture medium (Rm,Cm), and of the air gap (Ra,Ca) separating the upper electrode from the medium in the case of capacitive coupling. The internal resistance of the power supply was taken into account by insertion of a 50 Ω resistance. Capacitances and resistances of each RC-circuit have been calculated from geometry and material properties and they have been additionally determined experimentally: values of both methods are in good agreement. Calculation of the electrical parameters of the cell monolayer was based on the assumption that the monolayer consists of two parallel lipid layers covering the whole culture dish. A total capacitance Cm was attributed to the two facing lipid layers and a total of Rm to their inner resistance.
←

a Model HM8131-2 arbitrary function generator (HAMEG, Frankfurt a. M., Germany).

2.3. Calcium determination

For analysis of the calcium content the medium was decanted. Successively, the cell-matrix layer was washed with PBS and was treated with 4 ml of 0.1 N HCl in order to dissolve the mineral. Determination of calcium concentration was measured spectrometrically at 600 nm by using a colorimetric assay (Arsenazo III, Sigma–Aldrich) and a calcium-phosphorus containing standard solution (10 mg/dl, Sigma–Aldrich) for calibration.

2.4. Electron microscopy

Small pieces of culture dishes with adherent osteoblast-like cells were rapidly shock frozen in liquid nitrogen cooled propane and freeze-dried at −80°C for 3 days. The dried cell cultures were warmed up slowly and were either covered with a 20-nm carbon layer in a sputter coater (Edwards) for energy dispersive X-ray (EDX)-microanalysis or with a 3-nm chrome layer in a GATAN evaporator for scanning electron microscopical investigation. Element analysis was conducted on a Jeol scanning electron microscope (SEM) equipped with an energy dispersive X-ray (EDX) microprobe device (Roentec). An acceleration voltage of 20 kV was applied. For morphological imaging, a field effect SEM (LEO 982) was used applying an acceleration voltage of 0,8–2 kV.

For ultrastructural analysis, cryofixed and freeze dried cell-matrix layers were collected, vacuum-embedded in araldite resin and polymerised at 65°C. Transmission electron microscopy (TEM) and electron diffraction analysis (EDA) of ultrathin sections were carried out on a Philips CM 10 transmission electron microscope.

2.5. Statistical analysis

Means and standard deviations (S.D.) were calculated for descriptive statistical documentation. The unpaired Student's *t*-test was applied for analytical statistics. A value $P < 0.05$ was considered significant.

3. Results

3.1. Cultures stimulated by capacitively coupled electrical pulses

Seven days after plating, cells had reached a confluent state and electrical stimulation was started. At this time and on day 21, the cell-matrix layer of stimulated cultures and of controls showed similar AP activity and they clearly expressed procollagen type I, collagen type I, osteocalcin, osteonectin, and bone sialoprotein, whereas collagen type II was not detected. The different appearance of mineral crystals with a time dependent acceleration of mineral formation in electrically stimulated cultures is shown by

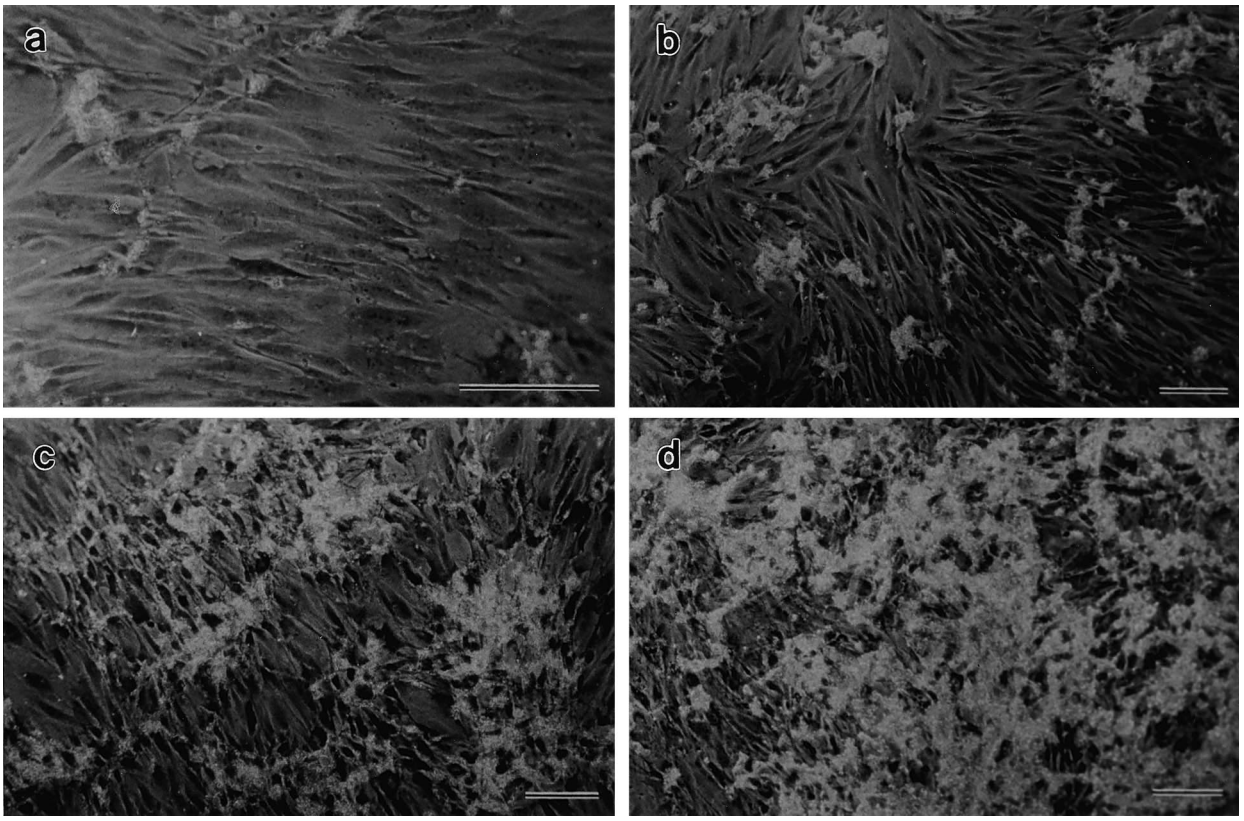

Fig. 2. Phase contrast micrographs of stimulated osteoblast-like cells by capacitively coupled electric fields at four different stages of mineralization. Stage I (7 days) represents the onset of mineralization (top, left). In stage II (10 day), small and sporadically distributed mineralized areas are visible (top, right). In stage III (14 days), the mineralized areas occupy 10–50% of the total culture dish area (bottom, left). In stage IV (21 days), more than 50% of the total culture dish area is covered by newly formed biomineral (bottom, right). Bars = 25 μm.

light microscopical images in Fig. 2. The osteoblast-like cells were confluent and displayed flattened cell bodies with bipolar processes. In control cultures only a few mineral deposits were visible.

In order to examine the effect of electrical stimulation on mineral metabolism of osteoblast-like cells, the total content of calcium was determined in stimulated cultures and in control cultures (Fig. 3). Before starting stimulation, calcium content of stimulated cultures and control cultures, was low and did not differ significantly. However after starting stimulation (days 10–21), a marked accumulation of calcium was detected. The stimulated cultures showed a significant increase of calcium content compared to controls indicating an enhanced mineral formation by osteoblast-like cells.

Observation of mineralizing cell cultures at different magnifications by SEM revealed areas of globular mineral deposition (mineral spherules) that were

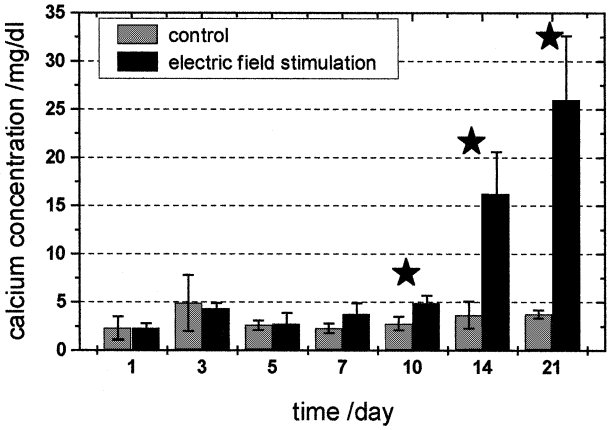

Fig. 3. Calcium content of cell-matrix layers. Capacitively coupled electric field stimulation was compared with non stimulated control cultures. Bars represent the means ± standard deviation (S.D.) of five different cultures; significantly different values between stimulated and control cultures are marked by an asterisk ($P < 0.01$).

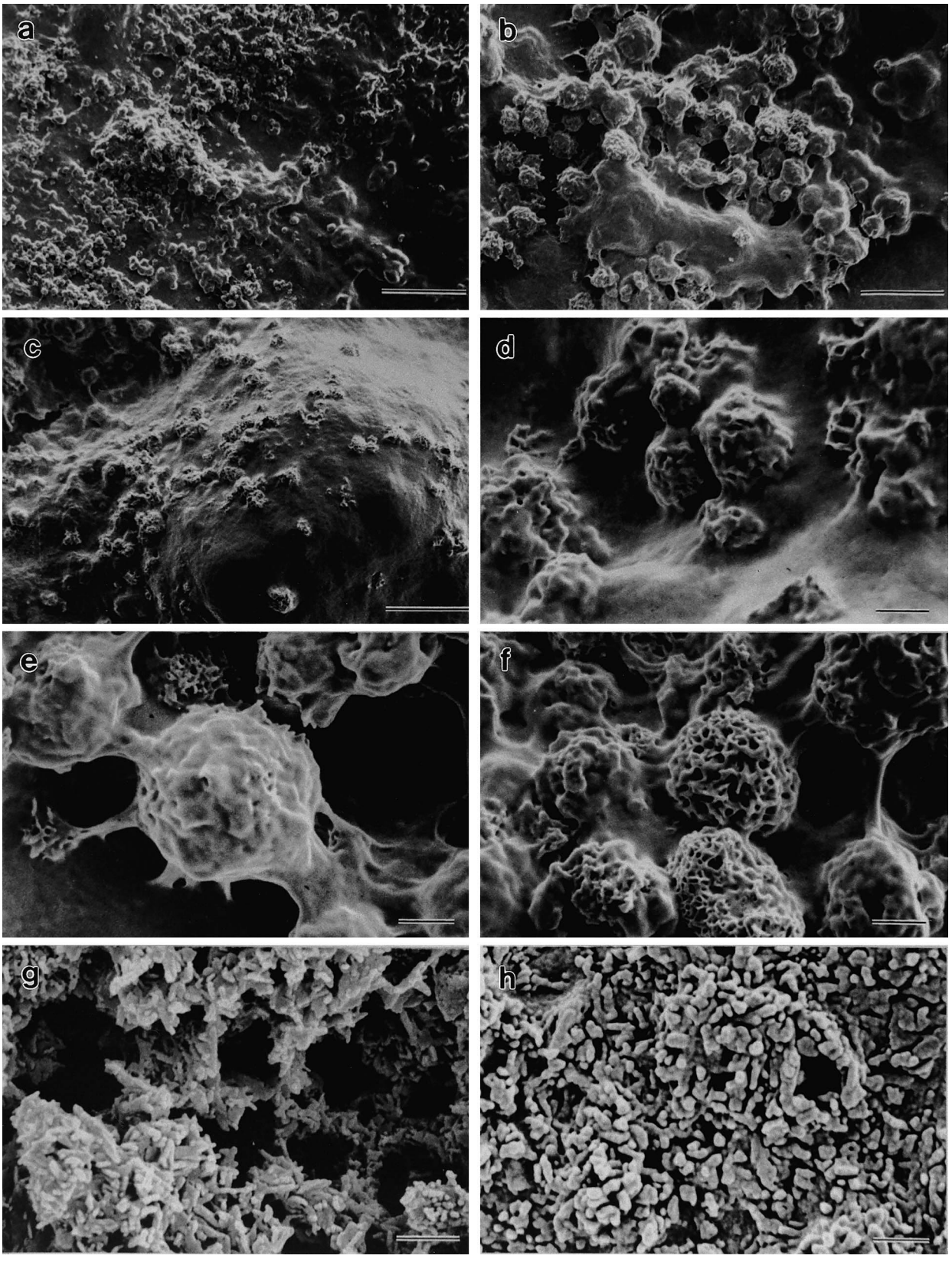
a
b
c
d
e
f
g
h

Fig. 4. Scanning electron micrographs of osteoblast-like cells stimulated by either capacitively (a–f) or semi-capacitive (g–h) coupled electric fields for a total of 2 weeks. (a) Survey of a mineralizing culture (bar = 10 μm). (b) Higher magnification of a region with mineral spherules beside an osteoblast-like cell (asterisk) (bar = 2 μm). (c,d) Newly formed nodules covering the cell surface (bars: c = 2 μm, d = 0.25 μm). (e) Mineral spherules in contact with a cellular membrane (bar = 0.25 μm) and (f) separated from the cell margin (bar = 0.25 μm). (g,h) Rod-shaped crystals in cultures after semi-capacitively coupled electric pulse stimulation (bars: g = 0.5 μm, h = 0.25 μm).
←

interspersed among the osteoblast-like cells (Fig. 4a) in stimulated cultures. Small mineral nodules with an approximate diameter of 200 nm were found as early indicators of newly formed biomineral in direct contact to the cell surface (Fig. 4c,d). In successive stages of mineralization, mineral spherules with a diameter of up to 700 nm appeared to surround the cells (Fig. 4b). These matured spherules were partly covered by cell membranes (Fig. 4e) or were found to occur with a clear distance from the cell margins (Fig. 4f). In control cultures quantity of mineral deposition was found to be lower than in stimulated cultures but morphology of mineral formations was found to be similar.

EDX analysis of stimulated cultures and control cultures revealed, that mineral spherules were rich in calcium and phosphorus (Fig. 5). Moderate amounts of sodium, potassium and sulfur were also detectable, whereby sodium and potassium, are constituents of the medium and the washing solution and may have been bind to the extracellular matrix or the cell surfaces. Instead, sulfur is indicative of sulfated proteoglycans.

Transmission electron microscopy of stimulated cultures and control cultures revealed typical nodules (Fig. 6a) similar to those found in in vivo osteogenesis with diffuse electron diffraction patterns (Fig. 6c), indicating strong lattice disorder of the crystals.

3.2. Cultures stimulated by semi-capacitively coupled electrical pulses

Light microscopy revealed that in cultures stimulated by semi-capacitively coupled electric pulses, cell morphology did not differ from that found after capacitive coupled stimulation however, a high amount of mineral deposition was obvious. By SEM and TEM observation, rod-shaped mineral crystals (thickness: 30–50 nm; length: 500 nm) were found to cover the surface of mineralized areas of the cultures (Figs. 4g,h and 6b) and displayed less diffuse and textured diffraction patterns (Fig. 6d) indicating coarse crystals with a high degree of crystallinity.

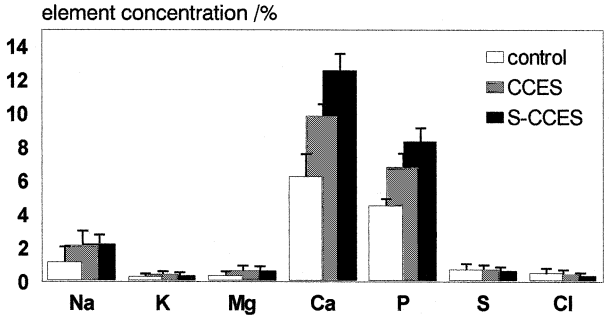

Fig. 5. Diagram showing elemental concentrations measured by EDX-analysis in mineralized cell cultures after 21 days (1 week without stimulation and 2 weeks with stimulation). Control, non-stimulated cultures; CCES, continuously stimulated cultures by capacitive coupled electric pulses; S-CCES, continuously stimulated cultures by semi-capacitive coupled electric pulses. Number of cultures was four; ten different culture areas (200×140 μm) were analyzed on each culture dish. Bars represent standard deviation of the mean.

4. Discussion

Osteoblasts control bone growth by active involvement in extracellular bone matrix formation and mineralization. Characterization of bone cells in vitro is based on the detection of different osteoblast markers such as alkaline phosphatase [17], collagen type I, osteocalcin, osteonectin [18], and bone sialoprotein whereas the absence of collagen type II exclude the presence of chondrocytes. Our immunohistochemical analysis identified the investigated cells as osteoblast-like cells.

In order to reveal possible mechanisms of the biomineralization process controlled by osteoblast-like cells in vitro that are triggered by specific electrical stimulation, a detailed description of the physical parameters is required. Since the electrical resistances

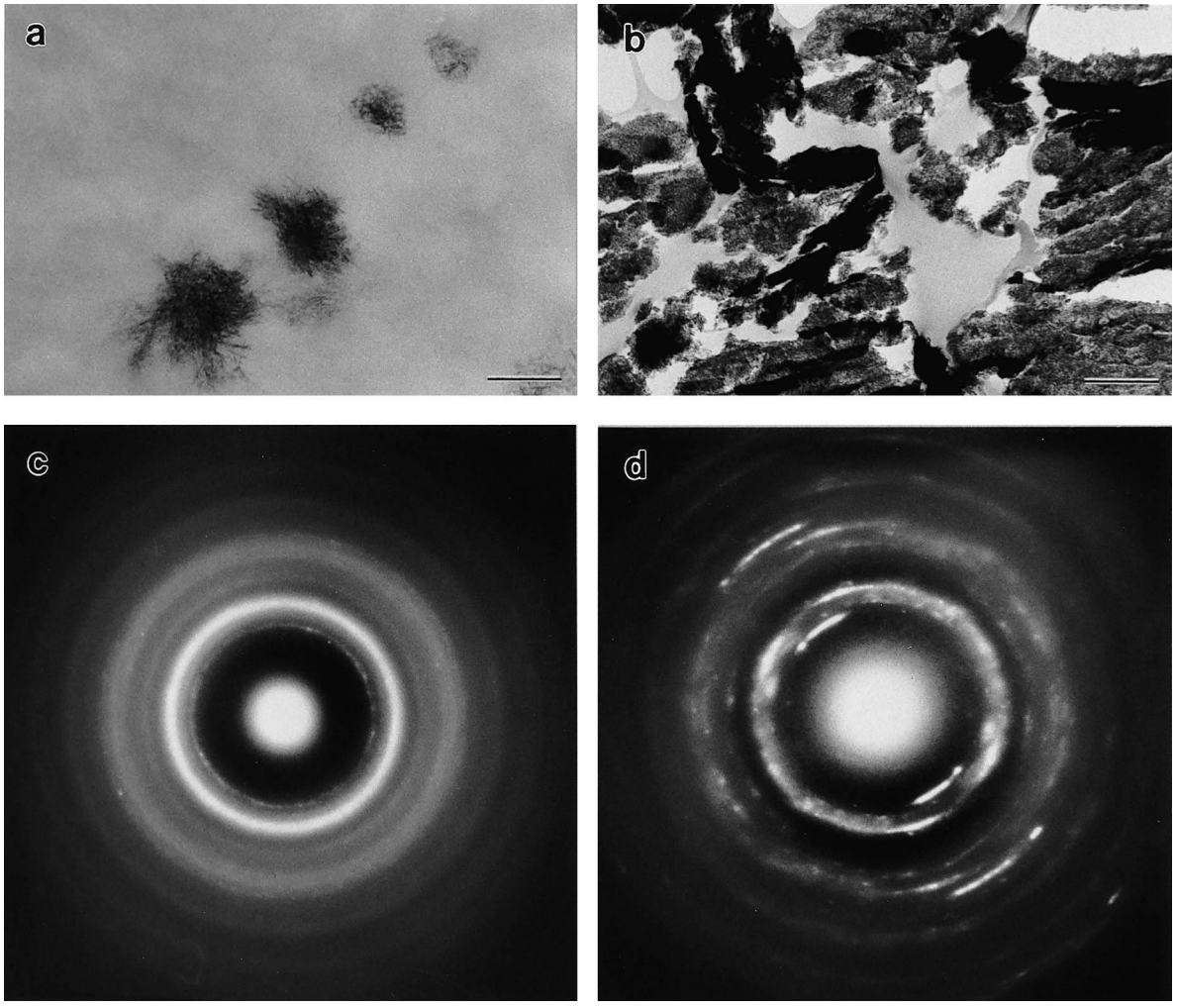

Fig. 6. TEM images of osteoblast-like cells stimulated for a period of 2 weeks. (a) Crystal nodules in capacitively stimulated cultures and in control cultures; osteoblasts are not visible due to omission of staining at the cryofixation (bar = 100 nm). The diffraction pattern shows a diffuse ring scattering of an apatitic mineral (c). (b) Large crystals formed after semi-capacitive stimulation of cultures (bar = 200 nm). The sparsity of diffracted electrons is indicative of large apatite crystal size, corresponding to the imaged crystal (d).

of culture dish and air gap are much higher than the resistances of medium and cell membranes, application of an external electric field results in a major voltage drop across the air gap and the culture dish (see Fig. 1B). Additionally, since the resistance of the cell monolayer is 100 times higher than the resistance of the medium, a considerable voltage drop occurs only across the cell monolayer. For example, having induced charges by the electric field across the cell monolayer at time $t=0$, the relaxation time τ is given by $\rho\ (t) = \rho_0 \times e^{-\sigma t/\varepsilon_0 \varepsilon} = \rho_0 \times e^{-t/\tau}$ where ρ_0 is the free charge density at $t=0$, ε_0 is the vacuum dielectric constant, ε is the dielectric constant of the monolayer and σ is the specific conductance of the monolayer. Using $\varepsilon_0 = 8.85 \times 10^{-12}$ F/m, $\varepsilon \approx 9.0$ [19] and $\sigma = 1.2 \times 10^{-7}\ \Omega^{-1}\,m^{-1}$, the calculated relaxation time is $\tau = \varepsilon_0 \varepsilon / \sigma = 6.5 \times 10^{-4}$ s. This means that a static electric field will fall to 1/e of its initial value within 650 μs. Therefore, a saw-tooth voltage with a step rising flank was chosen as input signal in order to generate voltage peaks with an uniform polarity across the cell monolayer. A repetition rate of 16 Hz was chosen because many molecular processes and carrier systems are sensitive to this range of frequency [12,20–22].

In cell-matrix layers a substantial calcium accumulation was only evident in stimulated cultures. The missing increase of calcium content in controls may

be due to a missing ascorbic acid component in the medium.

In addition to calcium quantification, the deposition of biomineral was evaluated morphologically. Investigations by SEM and TEM confirmed the analytical data revealed by EDX and EDA. EDX-analysis of the mineralizing cell-matrix layer in stimulated cultures and control cultures revealed a calcium to phosphorus ratio of 1.4, which is slightly lower than that of mineralizing bone. This finding may be explained by an increased level of phosphate compared to bone probably due to a higher cellular proportion in the cell-matrix layer. Although the content of sodium, potassium and magnesium has been found to be high in certain microareas at the mineralization front of different mineralizing tissues [23,24], the high concentrations of these elements found in the cell-matrix layer may strongly depend on the composition of the medium and on the washing procedure.

The diffraction pattern revealed that mineral deposits were composed of apatitic phases in all cultures. However, in cultures of the semi-capacitively coupled mode, the distortions of the crystal lattice were lower than in the more amorphous mineral deposits in cultures of the capacitively coupled mode and in the control cultures. Further, a striking difference concerning the morphology of the mineral phase was obvious. In cultures from the capacitively coupled mode and in the control cultures the mineral phase consisted of nodules and mineral spherules. Such globular mineralized bodies are typical for the onset of mineralization in vivo and are visible at the mineralization front of woven bone during early osteogenesis [25], in mantle dentin [26], in circumpulpal dentin [27,28], and in mineralizing cartilage during enchondral ossification [29]. Nodules are mineralized matrix vesicles and are considered as precursors of mineral spherules. Matrix vesicles are accepted to represent the sites of de novo mineral formation in vivo and in vitro with regard to their nucleational core complex responsible for mineral induction [30]. The early biomineralization of our osteoblast-like cells was associated with the formation of cell surface nodules with a diameter range comparable to that of matrix vesicles and nodules in vivo [31]. However, though collagen type I is clearly proofed in the culture a collagen related mineralization was not obvious. This in vitro system is similar to the initial mineral formation in vivo but it is limited concerning simulation of mature mineral formation in vivo.

The rod-shaped crystals identified in cultures stimulated by semi-capacitively coupled electric pulses showed dimensions of about 30–50 nm in width and about 500 nm in length. Similar large crystals have been observed in freeze-fracture samples of calcified cartilage [32] and in mineralizing primary cultures of avian growth plate chondrocytes [33]. These rod-shaped crystals are much larger than single hydroxyapatite biocrystals found in physiological calcified bone tissues. In SEM- and in TEM-images a characteristic substructure of the rod-shaped crystals, indicating a crystal–matrix relationship was not obvious. Thus, it seems likely that these crystals are mineral deposits formed by precipitation of electrolytes from the medium, which may have been induced by electrochemical effects of our system produced by the immersed electrode.

Our results demonstrate that the application of capacitively coupled electric fields allows the stimulation of bone cells by well-defined electric pulses eliminating possible electrolytic processes at the electrodes. Furthermore, physical stimulation of cell cultures for long terms is well suited to investigate the cascade of biochemical processes, resulting in a newly formed extracellular matrix which leads to biomineral formation. The results of the present study support the hypothesis, that stimulation of osteoblasts by capacitively coupled electric pulses can accelerate the multistep process of biomineralization in vitro.

Acknowledgements

We thank Mrs Grabiniok for her excellent technical assistance. Financial support by the German Bundesministerium für Bildung und Forschung, Biotechnologie 2000 and by co.don AG is gratefully acknowledged.

References

[1] J.H. McElhaney, J. Bone Joint Surg. 49A (1967) 1561–1571.
[2] C.A. Bassett, Calcif. Tissue Res. 1 (1968) 252–272.

[3] M. Akai, Y. Shirasaki, T. Tateishi, Arch. Phys. Med. Rehabil. 78 (1997) 405–409.
[4] C.T. Brighton, E. Okereke, S.R. Pollack, C.C. Clark, Clin. Orthop. 285 (1992) 255–262.
[5] M.A. Darendeliler, A. Darendeliler, P.M. Sinclair, Int. J. Adult Orthodon Orthognath. Surg. 12 (1997) 43–53.
[6] K.L. Grace, W.J. Revell, M. Brookes, Orthopedics 21 (1998) 297–302.
[7] P.S. Landry, K.K. Sadasivan, A.A. Marino, J.A. Albright, Clin. Orthop. 338 (1997) 262–270.
[8] T. Mohr, J.L. Andersen, F. Biering Sorensen, H. Galbo, J. Bangsbo, A. Wagner, M. Kjaer, Spinal Cord 35 (1997) 1–16.
[9] T. Mohr, J. Podenphant, F. Biering Sorensen, H. Galbo, G. Thamsborg, M. Kjaer, Calcif Tissue Int. 61 (1997) 22–25.
[10] R. Korenstein, D. Somjen, H. Fischler, I. Binderman, Biochim. Biophys. Acta 803 (1984) 302–307.
[11] J. Rubin, K.J. McLeod, L. Titus, M.S. Nanes, B.D. Catherwood, C.T. Rubin, J. Orthop. Res. 14 (1996) 7–15.
[12] H. Zhuang, W. Wang, R.M. Seldes, A.D. Tahernia, H. Fan, C.T. Brighton, Biochem. Biophys. Res. Commun. 237 (1997) 225–229.
[13] K. Heermeier, M. Spanner, J. Trager, R. Gradinger, P.G. Strauss, W. Kraus, J. Schmidt, Bioelectromagnetics 19 (1998) 222–231.
[14] Q. Wang, S. Zhong, J. Ouyang, L. Jiang, Z. Zhang, Y. Xie, S. Luo, Clin. Orthop. 348 (1998) 259–268.
[15] J. Wang, M.J. Glimcher, J. Mah, H.Y. Zhou, E. Salih, Bone 22 (1998) 621–628.
[16] S.J. Jones, A. Boyde, Cell Tissue Res. 184 (1977) 179–193.
[17] B. Herbert, A. Lecouturier, D. Masquelier, N. Hauser, C. Remacle, Calcif Tissue Int. 60 (1997) 216–223.
[18] E. Stringa, C. Filanti, D. Giunciuglio, A. Albini, P. Manduca, Bone 16 (1995) 663–670.
[19] R. Glaser, Biophysik, 4th ed., Fischer, Jena/Stuttgart, 1996.
[20] K.J. McLeod, H.J. Donahue, P.E. Levin, M.A. Fontaine, C.T. Rubin, J. Bone Miner. Res. 8 (1993) 977–984.
[21] R.J. Fitzsimmons, J.T. Ryaby, F.P. Magee, D.J. Baylink, Calcif. Tissue Int. 55 (1994) 376–380.
[22] R.J. Fitzsimmons, D.J. Baylink, Clin. Plast. Surg. 21 (1994) 401–406.
[23] H.P. Wiesmann, T. Tkotz, U. Joos, K. Zierold, U. Stratmann, T. Szuwart, U. Plate, H.J. Hohling, J. Bone Miner. Res. 12 (1997) 380–383.
[24] H.P. Wiesmann, U. Plate, K. Zierold, H.J. Hohling, J. Dent. Res. 77 (1998) 1654–1657.
[25] A. Boyde, J. Sela, Calcif. Tissue Res. 26 (1978) 47–49.
[26] U. Stratmann, K. Schaarschmidt, H.P. Wiesmann, U. Plate, H.J. Hohling, T. Szuwart, Anat. Embryol. Berl. 195 (1997) 289–297.
[27] H. Mishima, T. Sakae, Y. Kozawa, Scanning Microsc. 5 (1991) 723–728.
[28] H. Mishima, Y. Kozawa, Scanning 20 (1998) 235–236.
[29] A. Ornoy, Y. Langer, Isr. J. Med. Sci. 14 (1978) 745–752.
[30] L.N. Wu, T. Yoshimori, B.R. Genge, G.R. Sauer, T. Kirsch, Y. Ishikawa, R.E. Wuthier, J. Biol. Chem. 268 (1993) 25084–25094.
[31] H.C. Anderson, Clin. Orthop. 314 (1995) 266–280.
[32] T.K. Borg, R. Runyan, R.E. Wuthier, Anat. Rec. 199 (1981) 449–457.
[33] L.N. Wu, Y. Ishikawa, G.R. Sauer, B.R. Genge, F. Mwale, H. Mishima, R.E. Wuthier, J. Cell. Biochem. 57 (1995) 218–237.